Available online at www.sciencedirect.com
SCIENCE DIRECT®
Journal of Magnetic Resonance 172 (2005) 152–160
JMR Journal of Magnetic Resonance
www.elsevier.com/locate/jmr

A global inversion method for multi-dimensional NMR logging

Boqin Sun*, Keh-Jim Dunn

ChevronTexaco Energy Technology Company, 6001 Bollinger Canyon Rd, San Ramon, CA 94583, USA

Received 14 July 2004; revised 18 September 2004

Abstract

We describe a general global inversion methodology of multi-dimensional NMR logging for pore fluid typing and quantification in petroleum exploration. Although higher dimensions are theoretically possible, for practical reasons, we limit our discussion of proton density distributions as a function of two (2D) or three (3D) independent variables. The 2D can be diffusion coefficient and T_2 relaxation time (D–T_2), and the 3D can be diffusion coefficient, T_2, and T_1 relaxation times (D–T_2–T_1) of the saturating fluids in rocks. Using the contrast between the diffusion coefficients of fluids (oil and water), the oil and water phases within the rocks can be clearly identified. This 2D or 3D proton density distribution function can be obtained from either two-window or regular type multiple CPMG echo trains encoded with diffusion, T_1, and T_2 relaxation by varying echo spacing and wait time. From this 2D/3D proton density distribution function, not only the saturations of water and oil can be determined, the viscosity of the oil and the gas–oil ratio can also be estimated based on a previously experimentally determined D–T_2 relationship.

Keywords: NMR logging; Relaxation; Diffusion; Inversion

1. Introduction

Nuclear magnetic resonance (NMR) technology has been widely used in petroleum industry both in logging for oil exploration and in core analysis for petrophysical studies. NMR logging usually provides T_2 distributions of fluid-saturated earth formation obtained from Carr–Purcell–Meiboom–Gill (CPMG) [1] echo trains. The sum of the T_2 amplitudes at different relaxation times, when properly calibrated, is equal to the total porosity, which includes free fluid, and capillary and clay bound water. The proton population in solid phase is not included due to its short T_2 relaxation time and limitation of minimum inter-echo spacing that can be achieved at low field.

When multiple pore fluids, such as oil, gas, and water, are present, it becomes somewhat difficult to differentiate them, especially when their T_2 signals overlap. Earlier methods [2–4] use either different echo spacings, or different wait times, or combination thereof, for CPMG pulse sequences to obtain shifts or differences of T_2 distributions for hydrocarbon determination and sometimes for oil viscosity estimation. However, these methods are primarily set up in an one-dimensional framework where only the T_2 distribution is obtained. Whenever the T_2 signals are insensitive to such manipulations, the result of such analysis becomes ambiguous and sometimes inherently difficult when the T_2 signal of the oil overlaps with that of the capillary and clay bound water with short T_2 relaxation times.

Recent developments in 2D NMR [5–10] broaden the independent variables for proton density distribution function from the 1D of T_2 relaxation time to the 2D of diffusion coefficient and T_2 relaxation time (D–T_2). This expansion considerably improves the ability to differentiate oil and water in the (D–T_2) map of the proton density distribution function. Here, we describe the general methodology of multi-dimensional NMR logging

* Corresponding author.
E-mail address: bsun@chevrontexaco.com (B. Sun).

1090-7807/$ - see front matter © 2004 Elsevier Inc. All rights reserved.
doi:10.1016/j.jmr.2004.10.003

and present some of laboratory and logging measurement results in 2D of (D–T_2) and 3D of (D–T_2–T_1).

2. Theory

The echo amplitude of a CPMG measurement of a fluid-saturated porous medium in a uniform magnetic field has the following form

$$b_i = \sum_{j=1}^{m} a_j \exp(-t_i/T_{2j}) + \varepsilon_i, \quad i = 1, \ldots, n, \quad t_i = it_{\mathrm{E}}, \quad j = 1, \ldots, m, \tag{1}$$

where b_i is the ith echo amplitude, t_i is the decay time, T_{2j} is one of the m relaxation times which we assumed for the model equally spaced on a logarithmic scale, n is the number of echoes collected, t_{E} is the time between echoes, ε_i is the noise between data and the model, and a_j is the T_2 amplitude associated with the relaxation time T_{2j} to be solved by the inversion.

Eq. (1), when cast in integral form, is a Fredholm integral of the first kind:

$$b(t) = \int a(T_2) k_1(t, T_2)\, \mathrm{d}T_2 + \varepsilon, \tag{2}$$

where $k_1(t, T_2) = \exp(-t/T_2)$ is the kernel and $a(T_2)$ is the amplitude associated with the variable T_2 to be solved.

When the fluid-saturated formation is in a constant magnetic field gradient, the CPMG echo train with variable echo spacing and limited wait-time between scans is subjected to two additional kernels: one is to account for the extra decay caused by the molecular diffusion in an inhomogeneous magnetic field, and the other for the effect of insufficient polarization time for full spin alignment along the external B_0 field. Since we are dealing with a complicated system with a mixture of various fluids in a randomly distributed grain network, each kernel has to be associated with a distribution. Therefore, the time variation of CPMG echo train can be generalized from Eq. (2) to

$$b(t, \mathrm{TE}, \mathrm{WT}) = \iiint f(D, T_1, T_2) k_1(t, T_2) k_2(t, t_{\mathrm{E}}, D) k_3 \times (\mathrm{WT}, T_1)\, \mathrm{d}D\, \mathrm{d}T_1\, \mathrm{d}T_2 + \varepsilon, \tag{3}$$

where $f(D, T_1, T_2)$ denotes the three-dimensional proton density distribution function. The three kernels represent the time evolution of magnetization under T_1 and T_2 relaxation, and diffusion, which can be written as

$$k_1(t, T_2) = \exp(-t/T_2),$$
$$k_2(t, t_{\mathrm{E}}, D) = \exp\left(-\frac{1}{12}\gamma^2 g^2 t_{\mathrm{E}}^2 D t\right), \tag{4}$$
$$k_3(\mathrm{WT}, T_1) = 1 - \alpha \exp(-\mathrm{WT}/T_1),$$

where γ is the gyromagnetic ratio, g is the magnetic field gradient, and D is the diffusion coefficient of the pore fluid. Here, we assume that g is a constant both spatially and temporally. Hence, the kernel $k_2(t, t_{\mathrm{E}}, D)$ does not contain g as a variable. When g is not a constant spatially, its effect is usually folded in D, or if D of the single saturating fluid is known, g can be a variable in the kernel whose distribution can be solved. For convenience, we shall refer to k_1 as the T_2 kernel, k_2 as the D (diffusion) kernel, and k_3 as the T_1 kernel. Note that the T_1 kernel is also referred to as the polarization factor, where $\alpha = 2$ for the inversion recovery and $\alpha = 1$ for the saturation recovery type of pulse sequences.

The diffusion kernel, $k_2(t, t_{\mathrm{E}}, D) = \exp(-\frac{1}{12}\gamma^2 g^2 t_{\mathrm{E}}^2 D t)$, as it is written here, is treated as a base function for inversion. It is an approximation for the decay of CPMG echo signals caused by molecular diffusion in a gradient field. It is well known and has been discussed in many papers in the literature [11–13] that the diffusion decay in CPMG echo train is multiexponential and each echo has contributions from various coherence pathways. As pointed out by Hürlimann and Griffin [11], after the first few echoes, the diffusion kernel for the CPMG echo signals can be represented by an effective form of $\exp(-\frac{1}{12}\eta\gamma^2 g^2 t_{\mathrm{E}}^2 D t)$ where the factor η has a complicated dependence on the frequency offset ($\Delta\omega_0$), RF frequency (ω_1), and pulse parameters, and that $\eta = 1$ is a reasonably good approximation, considering the fact that the logging measurements are usually quite noisy and often masked by the presence of internal field gradients within the pore space of the rocks, which are comparable to the magnetic field gradients of the logging tool itself. In the following applications, we have assumed $\eta = 1$ and corrected the spin dynamics effect for the first two echo amplitudes [11] based on the field gradient map of the magnet.

The apparent T_1 or T_2 distribution takes into account (1) the bulk T_1 or T_2 properties of the fluid mixture, and (2) the surface-to-volume ratio of pores as well as the corresponding surface relaxation properties of the grains. The apparent diffusion distribution includes (1) the self-diffusion coefficients of the molecules of pore fluids, (2) the restricted diffusion effect for finite pore size, and (3) the internal field gradients caused by the susceptibility contrast between pore fluids and solid grains. The diffusion coefficients of the fluids and pore size distribution are the two types of key information that we would like to get from NMR logging. However, the ability to accurately extract these parameters is affected by the grain surface relaxation properties [14] and the presence of internal field gradients [15,16]. From previous studies, it is well known that the surface relaxivity for some carbonates is very small that their T_1 or T_2 distributions do not reflect the pore size distributions. The effect of internal field gradient induced by the susceptibility contrast between pore fluids and solid grains is not separable from

that of the diffusion. It is folded into the apparent diffusion coefficient distribution.

In Eq. (3), the T_1 kernel is not coupled with the other two kernels if the first echo is acquired at time $t = 0$. The other two kernels tangle together because of the common variable t. In practice, since the first echo always appears at $t = t_E$, all three kernels are related to each other if we simultaneously change echo spacing and wait-time. Following the general scheme for multi-dimensional NMR data acquisition, we need to develop pulse sequences to separate the tangled three kernels. The approaches in [5–9] are to separate T_2 and diffusion kernels by fixing the variable t in the diffusion kernel using two-window type modified CPMG pulse sequences with a very long wait-time between scans. Usually, the first window of this type of modified CPMG pulse sequences has either a fixed or known varied length, t_d, which fixes the t in the diffusion kernel, $k_2(t, t_E, D)$. In this first window, either the echo spacing t_E, or the pulsed field gradient amplitude, or the diffusion time Δ between the pulsed field gradients is varied, such that the diffusion information of fluids in the pore space is encoded. The second window usually is a regular CPMG pulse sequence with the smallest t_E possible to acquire such encoded information. When the t in the diffusion kernel $k_2(t, t_E, D)$ is fixed to be t_d and the T_1 kernel is reduced to one for a sufficiently long wait-time, Eq. (3) becomes:

$$b(t, t_E) = \int\int f(D, T_2) k_2(t_d, t_E, D) k_1(t, T_2)\, dD\, dT_2 + \varepsilon, \tag{5}$$

where the two kernels are now separated, and the inversion can be easily implemented to obtain a T_2 relaxation-diffusion 2D (RD2D) NMR display through the methods described in [5–9].

To obtain a T_1–T_2 2D NMR display, the first window is used to vary the T_1 recovery time for encoding T_1 relaxation decay while the second window is again a regular CPMG pulse sequence with the smallest echo spacing. The pulse sequence used in the first window is based on either inversion or saturation recovery method. In most NMR logging applications, we simply vary the wait-time between consecutive CPMG data acquisitions to encode T_1 evolution in the T_1 kernel. Since the diffusion does not affect the T_1 modulation in the first window and the diffusion effect is minimal in the second window due to short echo spacing, the diffusion kernel can be removed from Eq. (3), and the variation of the echo amplitude becomes

$$b(t, \mathrm{WT}) = \int\int f(T_2, T_1) k_3(\mathrm{WT}, T_1) k_1(t, T_2)\, dT_1\, dT_2 + \varepsilon. \tag{6}$$

Here, the T_1 and T_2 kernels are not tangled together. The 2D inversion is straightforward.

In fact, the separation of tangled kernels is really not essential, as long as the tangled kernels are treated as a single kernel for the direct one-step inversion of 2D/3D proton density distribution function. Thus, two-window type modified CPMG pulse sequences are really not necessary. The regular CPMG measurements with different echo spacings and wait-time will just be fine. In this scheme, the problem can be cast in a three-dimensional framework using a single kernel:

$$b(t, t_E, \mathrm{WT}) = \int\int\int f(T_1, T_2, D) k(t, t_E, \mathrm{WT}, T_1, T_2, D) \times dD\, dT_1\, dT_2 + \varepsilon. \tag{7}$$

In discrete form, Eq. (7) can be written as:

$$b_{iks} = \sum_{r=1}^{n} \sum_{j=1}^{m} \sum_{l=1}^{p} f_{rlj} \exp\left(-\frac{1}{12}\gamma^2 g^2 t_{E_k}^2 D_l t_i\right) \exp(-t_i/T_{2j}) \times (1 - \alpha \exp(-\mathrm{WT}_s/T_{1r})) + \varepsilon_{iks}, \tag{8}$$

where b_{iks} is the amplitude of ith echo using t_{E_k} and WT_s, and ε_{iks} is the noise. There are m T_2 relaxation times, n T_1 relaxation times, and p diffusion coefficients assumed by the model, all equally spaced on their respective logarithmic scales. Thus, to write Eq. (8) in simplified notation, we have:

$$b_{iks} = E_{iks,rlj} f_{rlj} + \varepsilon_{iks}, \tag{9}$$

where

$$i = 1, \ldots, NE_k, \quad k = 1, \ldots, q, \quad s = 1, \ldots, w, \quad r = 1, \ldots, n, \quad l = 1, \ldots, p, \quad j = 1, \ldots, m, \tag{10}$$

indicating that there were NE_k echoes collected for the run with t_{E_k}, q echo trains with different t_E's and w echo trains with different WTs. p is the number of pre-selected components of diffusion coefficients equally spaced on a logarithmic scale in the first dimension; m and n are the numbers of pre-selected components of T_2 and T_1 relaxation times, respectively, both equally spaced on a logarithmic scale in the second and third dimensions; b_{iks} is the amplitude of ith echo of the kth echo train using echo spacing t_{E_k} and wait time WT_s; and f_{rlj} is the proton amplitude at diffusion coefficient D_l, relaxation time T_{2j}, relaxation time T_{1r}, and

$$E_{iks,rlj} = \exp\left(-\frac{1}{12}\gamma^2 g^2 t_{E_k}^2 D_l t_i\right) \exp(-t_i/T_{2j}) \times (1 - \alpha \exp(-\mathrm{WT}_s/T_{1r})). \tag{11}$$

To solve Eq. (9) in a practical manner, each echo train can be compressed or averaged to several data bins, with the variance of the noise for each data bin properly taken care of as weighting factor for each corresponding data bin [17]. Thus, the large number of echoes can be reduced to a manageable number of data bins (say 30 data bins, typically). On a PC of 1 GHz, for a (D–T_2–T_1) map of $30 \times 30 \times 30$ with an input data of

nine echo trains with different echo spacings and wait-times, the computation takes about 5 min. The commonly used singular value decomposition (SVD) [18], or the Butler–Reeds–Dawson (BRD) method [19], or the combinations thereof, can be used in the usual manner by imposing the non-negativity constraint and ensuring the solution to be commensurate with the noise level. The methods for such kind of inversion have been discussed extensively in the literature [20–24].

When acquired data are sufficient, it is straightforward to reduce Eq. (9) from 3D to 2D inversion. For example, one can fix the wait-time and use only the diffusion and T_2 kernels to derive RD2D distributions from a set of CPMG echo trains with different echo spacing. One can also use the minimal echo spacing and vary the wait-time to obtain T_1–T_2 correlation distribution. The computation time reduces from 5 min for a 3D inversion to a few seconds for a 2D inversion. The major advantage of this global inversion scheme is that it greatly reduces the number of data acquisitions required to perform a 2D or 3D inversion. On the other hand, proper physical constraints may be necessary to constrain the solutions to reasonable ones, for example, $T_1 \geqslant T_2$.

Since the diffusion kernel and the T_1 kernel are not coupled, it is advantageous to solve the T_1–T_2 proton density distribution function first, and then to use the solution as input for solving the D–T_2 map. This should place some physical constraints on the inversion of D–T_2 distribution function and is also computationally more efficient. If this were the case, Eq. (9) can be written as

$$b_{iks} = \sum_{j=1}^{m}\sum_{l=1}^{p} f_{lj} \sum_{r=1}^{n} h_{jr} \exp\left(-\frac{1}{12}\gamma^2 g^2 t_E^2 D_l t_i\right) \exp\left(-t_i/T_{2j}\right) + \varepsilon_{iks} \tag{12}$$

and solved for f_{lj}, where

$$h_{jr} = h_j(T_{1r})(1 - \alpha \exp(-\mathrm{WT}_s/T_{1r})) \tag{13}$$

and $h_j(T_{1r})$ is the normalized 2D proton density distribution function solved earlier for the T_1–T_2 map, i.e., $\sum_r h_j(T_{1r}) = 1$.

3. Results and discussions

There are many ways to acquire raw data for 2D/3D inversion to obtain Relaxation-Diffusion 2D/3D NMR proton density distribution functions. For example, T_1 encoding is mainly based on either inversion or saturation recovery, T_2 relaxation is measured by CPMG pulse sequence, and diffusion effect is encoded by varying echo spacing or external magnetic field gradient. In the laboratory, sufficient data can always be acquired for proper inversion. However, in a logging environment limited by logging speed and fixed external field gradient distribution, the acquisition sequence has to be simple and efficient.

Fig. 1 shows two types of acquisition sequences mainly for logging situations: (A) regular CPMG versus (B) two-window modified CPMG, both in a constant field gradient. The wait-time variation between two successive excitations is used to encode T_1 information. In the regular CPMG acquisition mode, the diffusion effect is simply encoded and recorded by acquiring echo trains of different echo spacings. In the two-window modified CPMG acquisition mode, the diffusion effect is encoded in the first window by varying the echo spacing and recorded in the second window with a T_2 distribution of minimum echo spacing which minimizes the diffusion effect. In the following, we describe laboratory results of fluid-saturated glass beads of 0.45 mm diameter obtained from regular CPMG measurements, and field results of NMR logging, one from two-window and another one from regular CPMG measurements.

The laboratory experiments for 2D/3D NMR inversion were carried out using a MARAN Ultra instrument. To introduce a magnetic field gradient, we increased the gap between the two poles of an 11 MHz permanent magnet to 5 in. The resonance frequency at the center of the magnet reduces to 6 MHz and the size of the saddle point where the field is homogeneous is about 1 cubic inch. To calibrate the distributed gradient, we used a deionized water sample and measured a set of CPMG echo trains with $t_E = 0.3$, 0.6, 1.2, 2.4, 4.8, 9.6, and 19.2 ms, respectively. The wait-time was 12 s between scans, the 90° pulse length was 18 μs, and the refocusing pulse length was 27 μs for maximum echo intensity. The water temperature was 28 °C and its diffusion coefficient should be 2.4×10^{-5} cm^2/s. Using Eq. (9), we performed a relaxation-diffusion 2D inversion and determined the field gradient distribution which has a logarithmic mean of about 20 G/cm. We then sat-

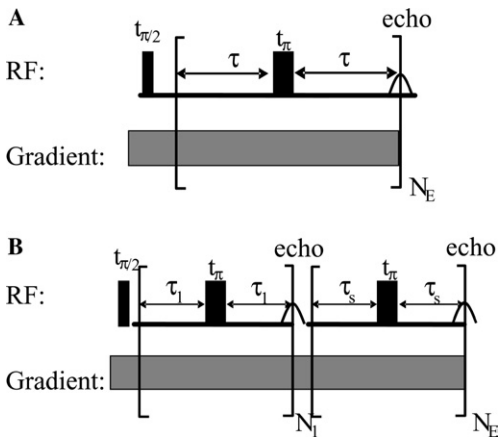

Fig. 1. (A) Using different echo spacing and a constant field gradient in a regular CPMG for encoding, and (B) constant field gradient and two-window CPMG for encoding.

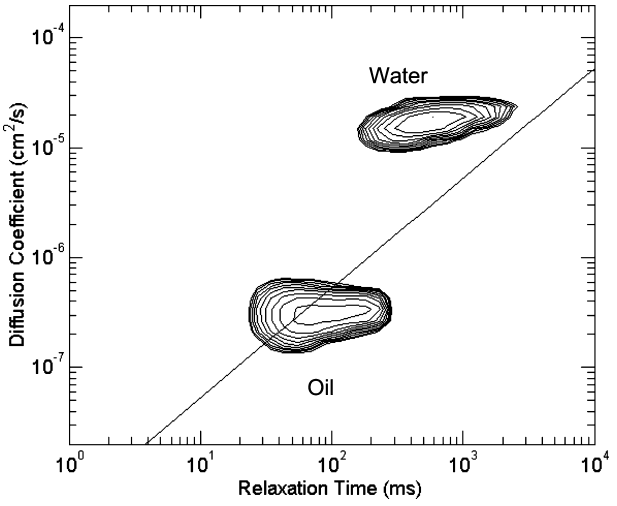

Fig. 2. RD2D experimental results of a water–oil saturated glass bead pack. The inversion clearly separates water and white oil. The wide feature of the oil peak indicates that white oil is a mixture. The seven TE values were 0.3, 0.6, 1.2, 2.4, 4.8, 9.6, and 19.2 ms. The wait-time between scans was 12 s. CPMG echo train data were acquired on a 6 MHz modified MARAN Ultra spectrometer.

urated a glass bead pack with a mixture of water and white oil, and measured another set of CPMG echo trains with the same t_E values. The volume ratio of water and white oil is about 1:1. Fig. 2 shows the RD2D contour plot derived from our inversion algorithm with a D/T_2 line, plotted diagonally, for dead oils established experimentally in the laboratory [25]. It clearly shows the water and oil peaks. The diffusion coefficient of water is found to be 2.0×10^{-5} cm^2/s, while the diffusion coefficient of the white oil spreads out and its logarithmic mean, situated on the D/T_2 line, is about 6×10^{-7} cm^2/s. Both are close to our expectation.

For 3D inversion of a similar fluid-saturated glass bead pack, we introduce T_1 variation with different wait times. A total of 10 echo trains were acquired with t_E and wait time pair as follows: (0.6 ms, 10 s), (0.6 ms, 1 ms), (0.6 ms, 10 ms), (0.6 ms, 100 ms), (0.6 ms, 1 s), (1.2 ms, 10 s), (2.4 ms, 10 s), (4.8 ms, 10 s), (9.6 ms, 10 s), and (19.2 ms, 10 s). Fig. 3 shows (A) the 3D plot of (D–T_2–T_1) derived from our inversion as well as the projections in (B) D–T_1, (C) D–T_2, and (D) T_1–T_2

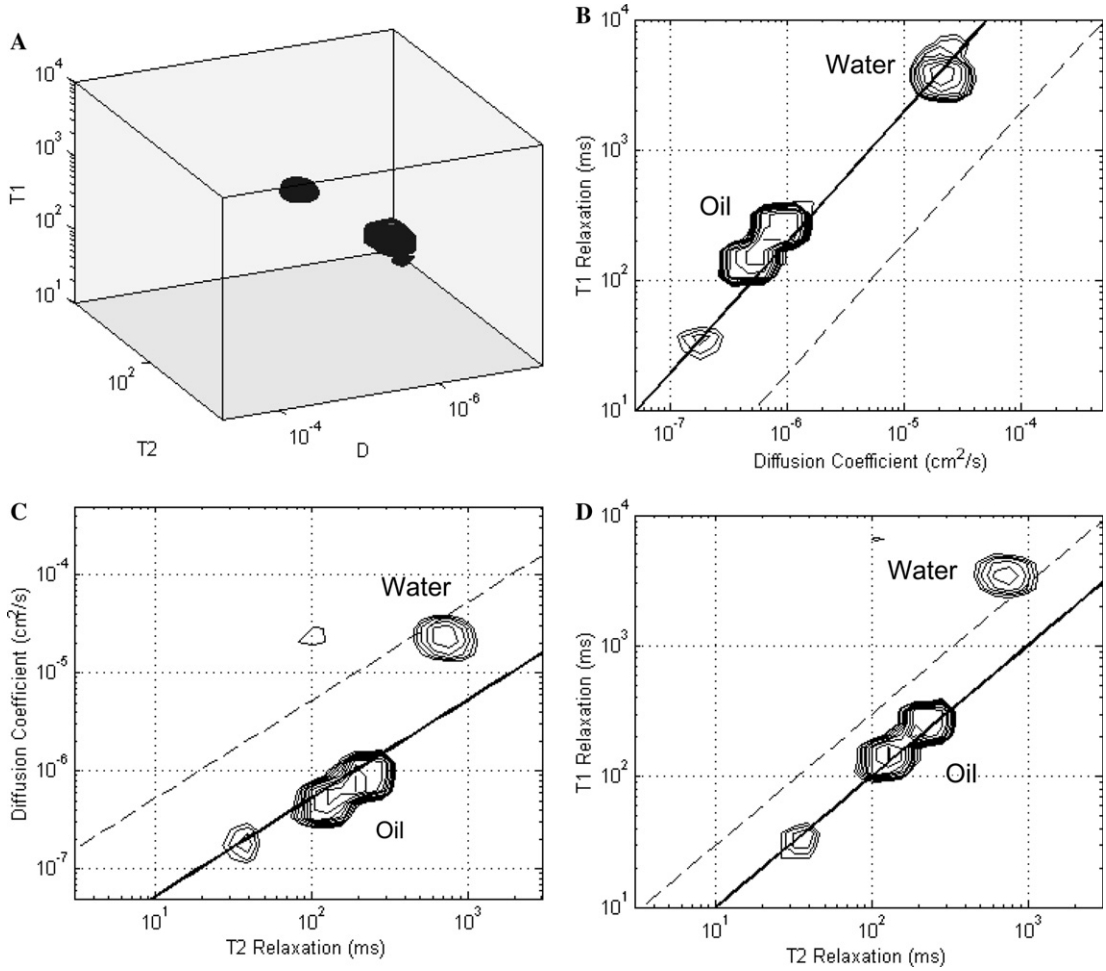

Fig. 3. 3D inversion of experimental results of a water–oil saturated glass bead pack. From which the diffusion constants of oil and water, T_1/T_2 ratios, become transparent. CPMG echo train data were acquired on a 6 MHz modified MARAN Ultra spectrometer.

domains. It clearly shows the water and oil peaks in the display. The diffusion coefficient of water is still close to 2.0×10^{-5} cm^2/s, and the diffusion coefficient of the white oil spreads out with a logarithmic mean also of about 6×10^{-7} cm^2/s. From the T_1–T_2 map, we see that the ratio of T_1/T_2 for the oil peak is roughly about 1 while the ratio for the water peak is more than 3 as indicated by the dashed line. The T_1/T_2 ratio for water signal is related to the ratio of the surface relaxivity, ρ_1/ρ_2, where ρ_1 and ρ_2 are the surface relaxivities for T_1 and T_2, respectively. Note that there are some spurious peaks in the display due to inversion error.

There is a small modification to the T_1 kernel in the above 3D inversion program. This is because the first five CPMG echo trains with same t_E but different wait times were acquired in single shot. As was pointed out in [11], the CPMG sequence is very much like a spin-locking experiment where the total magnetization is locked along an axis that is slightly away from the y-axis in the yz plane if the 90° pulse is applied along the x axis and refocusing pulses are along the y axis. This implies that at the end of each CPMG sequence, there is already a small z-component, which is a projection of the spin-locked magnetization. As the wait-time decreases to zero, the first echo intensity reduces to a finite value instead of zero, due to the presence of this small z-component. This is clearly indicated in Fig. 4. To account for this effect, the T_1 kernel has to be modified to

$$k_3(\mathrm{WT},T_1)=\beta+(1-\beta)(1-\exp(-\mathrm{WT}_s/T_{1r})). \qquad (14)$$

Numerical simulation shows that this small z-component, β, can be as large as 15% of the total echo intensity depending upon the B_0 field gradient distribution and RF field strength. To fit our experiment results, we found that β has to be about 0.12 which is similar to the number used for correction of T_2 decay, i.e., $\langle n_z^2\rangle$, in [11]. It should be emphasized, however, that such modification (Eq. (14)) is not necessary when full polarization is attained before the 90° pulse.

3D inversion is usually much slower than 2D inversion. Since T_1 and diffusion encoding can be done separately and there is no coupling between them, we can first run a T_1–T_2 2D inversion using data with minimum echo spacing such that the diffusion effect is minimized. We then use the T_1–T_2 map as a constraint to perform D–T_2 inversion with the rest of the data acquired at different t_E's. Fig. 5 shows the results of T_1–T_2 and D–T_2 maps derived from the same data set of Fig. 3 with this two-step method. The T_1/T_2 ratios for oil and water peaks are similar to those in Fig. 3. The D–T_2 distribution is more dispersed than those given by the 3D inversion possibly due to different degrees of regularization.

Our 2D/3D NMR inversion has also been applied to NMR logging data. The 2D/3D inversion results can be

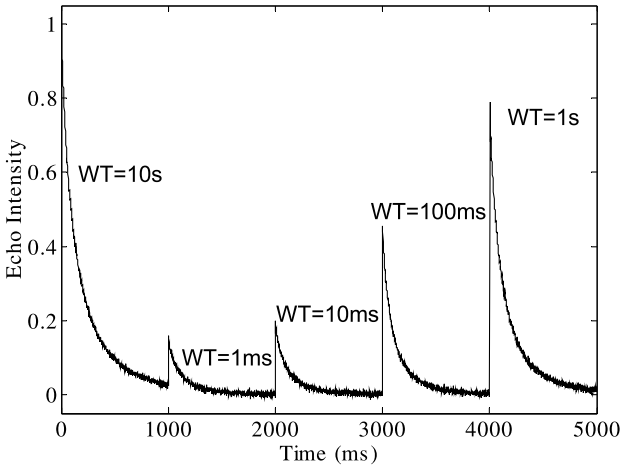

Fig. 4. The projection of the spin-locked magnetization during a CPMG sequence in a sequential excitation gives a small z-component in the T_1 kernel at the limit of 0 wait time.

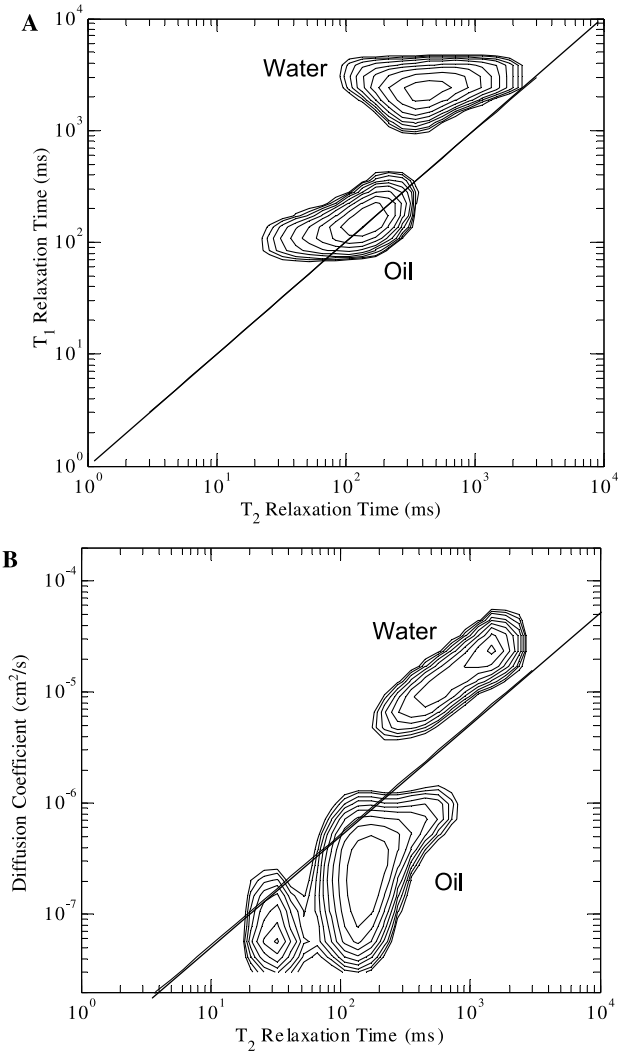

Fig. 5. (A) T_1–T_2 2D distribution and (B) D–T_2 distribution derived from the same set of data as that in Fig. 3 with a two-step 2D inversion method as an alternative for direct 3D inversion.

obtained as a function of depth (i.e., the distance from the surface to the tool location where the measurement was made). The two examples we show are one for the two-window type CPMG measurements (diffusion editing), and another one for the regular CPMG measurements. Both types of logging tools can operate at multiple frequencies in a dipole field with well-defined field gradient values.

Fig. 6 shows the result of a 3D inversion from a diffusion-editing measurement. Based on the formation temperature and temperature behavior of diffusion coefficients of oil and water [25], we assign the peak on the D/T_2 line as the oil and the other peak as the water peak. This assignment was further corroborated with information obtained from other logs. A constraint of $0.8T_1 > T_2$ was placed for the inversion. The inversion result from such a simple constraint is very satisfying because it shows the D–T_1 map as a simple combination of D–T_2 and T_1–T_2 maps, reflecting the fact that there is no coupling between D and T_1. Without such a constraint, the results are more spurious. Naturally, when the acquired data are sufficient, the two-step inversion (T_1–$T_2 \rightarrow D$–T_2) should place more constraints and should be more efficient computationally. Note that for the diffusion-editing sequence, the diffusion decay encoded in the first window is a weighted average of a direct echo and a stimulated echo with different decay rates [8], which needs to be properly taken care of.

Fig. 7 shows another example of 2D NMR logging result using regular CPMG measurements with different t_E's, where frames A, B, C, and D depict the D–T_2 map of decreasing depths from water zone (A and B) to oil zone (C and D). Note that peaks corresponding to the free fluid and capillary bound water are clearly seen in the water leg. When oil zone is reached, additional oil peak emerges at the upper right-hand corner. Using relationship between T_2 relaxation time (or diffusion coefficient) and oil viscosity [25], we should be able to estimate oil viscosity and gas–oil ratio from a RD2D distribution.

4. Conclusions

We described a global inversion scheme for obtaining a two- or three-dimensional NMR proton distribution

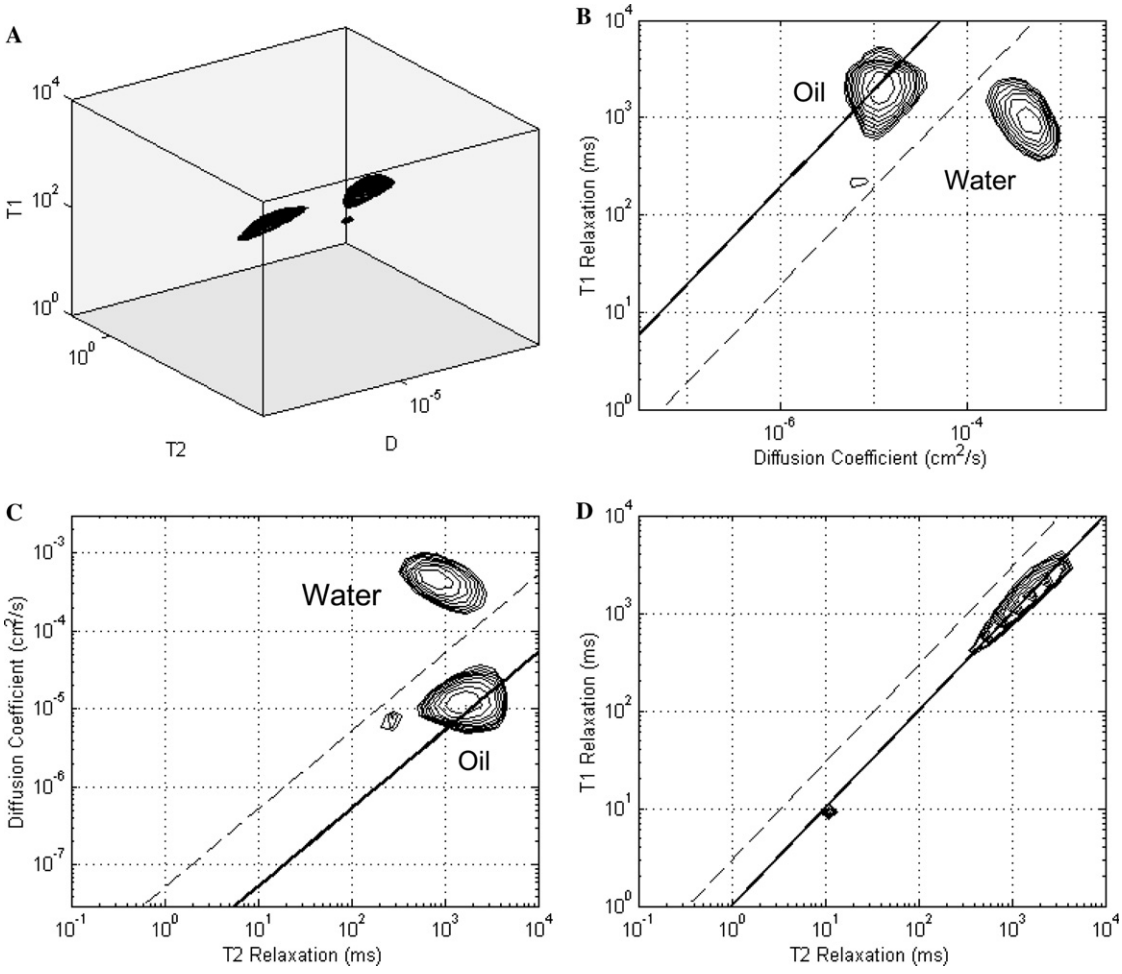

Fig. 6. A field example of 3D inversion of a two-window type CPMG measurement. The proton density distribution clearly separates oil from water.

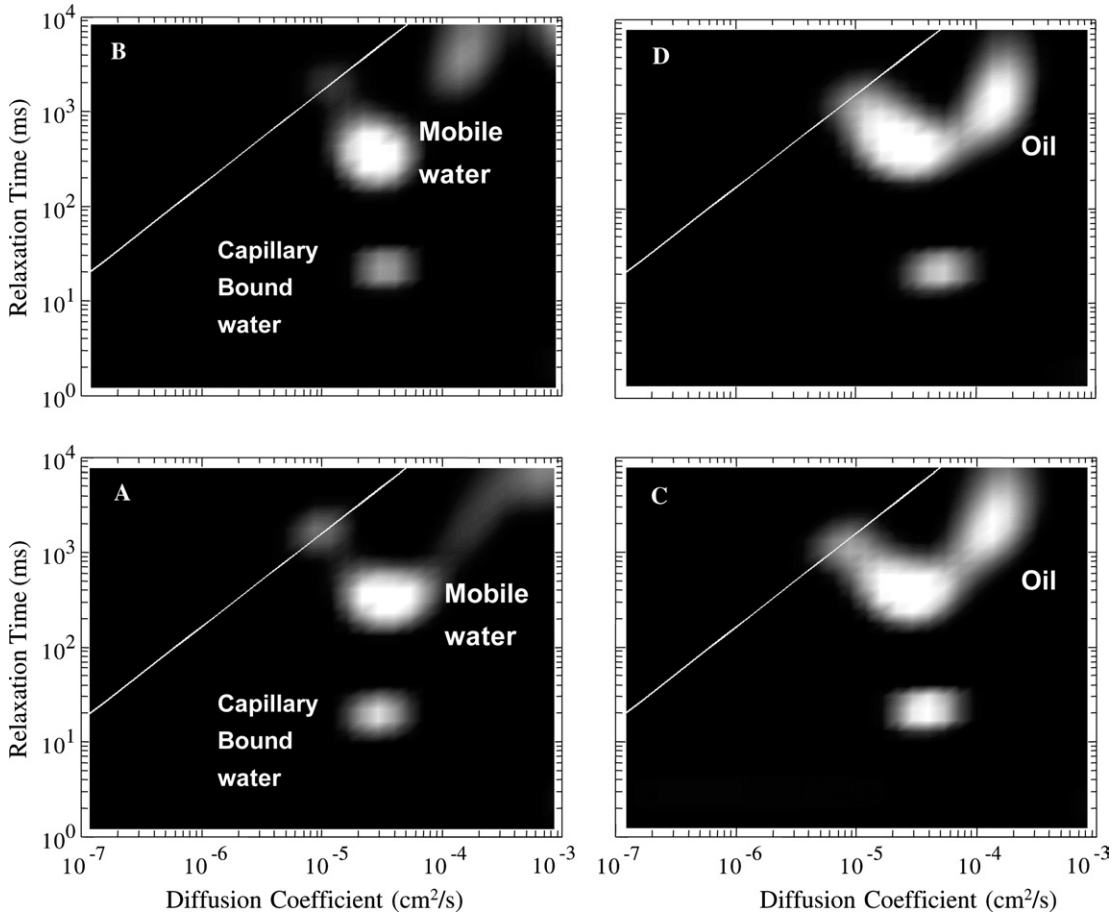

Fig. 7. Another 2D NMR logging example obtained with regular CPMG measurements, where frames A, B, C, and D show the D–T_2 map as the depth (i.e., the distance from the surface to the tool location where the measurement was made) is decreasing from a water zone (A and B) into an oil zone (C and D). The solid line (white) indicates the D–T_2 relation for dead oils at ambient condition.

function using either the regular CPMG pulse sequences or the two-window type CPMG measurements. Whenever acquired data are sufficient, the 3D inversion can be reduced to a two-step 2D inversion to reduce computation time. The first step gives a T_1–T_2 distribution using multiple echo trains with different wait times and minimum echo spacing that minimizes the diffusion effect. The second step yields a D–T_2 distribution using additional echo trains with different echo spacings and wait times under the constraints given by the T_1–T_2 distribution.

We also briefly outlined two data acquisition schemes for NMR logging. When we use a single shot to correct data for T_1 inversion, the T_1 kernel has to be modified to account for steady-state limitation.

Preliminary laboratory and field test results show that 2D/3D NMR logging provides multiple formation and fluid properties such as porosity, oil and water saturation, oil viscosity, permeability, and wettability. It is a very important analytical tool for oil exploration and can be used for other industries such as food characterization.

Acknowledgments

The authors thank Ron Cherry and his colleagues of Halliburton and Nick Heaton and Nate Bachman of Schlumberger for assisting us in log data acquisition and providing us the necessary information on data format. They also thank the ChevronTexaco management for supporting and giving permission to publish this work.

References

[1] H.Y. Carr, E.M. Purcell, Phys. Rev. 94 (1954) 630;
S. Meiboom, D. Gill, Rev. Sci. Instrum. 29 (1958) 668.
[2] R. Akkurt, H.J. Vinegar, P.N. Tutunjian, A.J. Guillory, The Log Analyst 37 (1996) 33.
[3] S. Chen, D.T. Georgi, E.M. Withjack, C. Minetto, O. Olima, H. Gamin, Petrophysics 41 (2000) 33.
[4] R. Freedman, A. Sezginer, M. Flaum, A. Matteson, S. Lo, G.J. Hirasaki, SPE Paper 63214, Society of Petroleum Engineers, Dallas, TX, 2000.
[5] L. Venkataramanan, Y-Q. Song, M.D. Hürlimann, Solving Fredholm integrals of the first kind with tensor product structure in 2 and 2.5 dimensions, IEEE Trans. Signal Process. 50 (2002) 1017–1026.

[6] M.D. Hürlimann, L. Venkataramanan, Quantitative measurement of two-dimensional distribution functions of diffusion and relaxation in grossly inhomogeneous fields, J. Magn. Reson. 157 (2002) 31–42.
[7] Y.-Q. Song, L. Venkataramanan, M.D. Hürlimann, M. Flaum, P. Frulla, C. Straley, T_1–T_2 correlation spectra obtained using a fast two-dimensional Laplace inversion, J. Magn. Reson. 154 (2002) 261–268.
[8] M.D. Hürlimann, L. Venkataramanan, C. Flaum, P. Speier, C. Karmonik, R. Freedman, N. Heaton, Diffusion-editing: new NMR measurement of saturation and pore geometry, in: SPWLA Proceedings of the 43rd Annual Logging Symposium, Oiso, Japan, Paper FFF, 2002.
[9] B. Sun, K.-J. Dunn, Probing the internal field gradients in porous media, Phys. Rev. E 65 (2002) 051309.
[10] B. Sun, K.-J. Dunn, B.J. Bilodeau, S.W. Stonard, M.A. Al-Rushaid, Two-dimensional NMR logging and field test results, in: SPWLA 45th Annual Symposium, Paper KK, June 6–9, 2004.
[11] M.D. Hürlimann, D.D. Griffin, Spin dynamics of Carr–Purcell–Meiboom–Gill sequences in grossly inhomogeneous B_0 and B_1 fields and application to NMR well logging, J. Magn. Reson. 143 (2000) 120–135.
[12] R. Kaiser, E. Bartholdi, R.R. Ernst, Diffusion and field-gradient effects in NMR Fourier spectroscopy, J. Chem. Phys. 60 (1974) 2966–2979.
[13] G. Goelman, M.G. Prammer, The CPMG pulse sequence in strong magnetic field gradients with applications to oil-well logging, J. Magn. Reson. A 113 (1995) 11–18.
[14] K.R. Brownstein, C.E. Tarr, Phys. Rev. A 19 (1979) 2446.
[15] D.J. Bergman, K.-J. Dunn, NMR of diffusing atoms in a periodic porous medium in the presence of a nonuniform magnetic field, Phys. Rev. E 52 (1995) 6516–6535.
[16] M.D. Hürlimann, Effective gradients in porous media due to susceptibility differences, J. Magn. Reson. 134 (1998) 232–240.
[17] R. Freedman, U.S. Patents 5,291,137 (1994) and 5,381,092 (1995).
[18] See, for example W.H. Press, S.A. Teukolsky, W.T. Vetterling, B.P. Flannery, Numerical Recipes, Cambridge University Press, 1992.
[19] J.P. Butler, J.A. Reeds, S.V. Dawson, Estimating solutions of the first kind integral equations with non-negative constraints and optimal smoothing, SIAM J. Numer. Anal. 18 (1981) 381–397.
[20] M.D. Silva, K.G. Helmer, J-H. Lee, S.S. Han, C.S. Springer Jr., C.H. Sotak, Deconvolution of compartmental water diffusion coefficients in yeast-cell suspension using combined T_1 and diffusion measurements, J. Magn. Reson. 156 (2002) 52–63.
[21] S.W. Provencher, A constrained regularization method for inverting data represented by linear algebraic or integral equations, Comput. Phys. Commun. 27 (1982) 213–227.
[22] S.W. Provencher, CONTIN: A general purpose constrained regularization program for inverting noisy linear algebraic or integral equations, Comput. Phys. Commun. 27 (1982) 229–242.
[23] J-H. Lee, C. Labadie, C.S. Springer, G.S. Harbison, Two dimensional inverse Laplace transform NMR: altered relaxation times allow detection of exchange correlation, J. Am. Chem. Soc. 115 (1993) 7761–7764.
[24] A.E. English, K.P. Whittall, M.L.G. Joy, R.M. Henkelman, Quantitative two-dimensional time correlation relaxometry, Magn. Reson. Med. 22 (1991) 425–434.
[25] S.-W. Lo, G. Hirasaki, W.V. House, R. Kobayashi, Correlations of NMR relaxation times with viscosity, diffusivity, and gas/oil ratio of methane/hydrocarbon, SPE Paper 63217, Society of Petroleum Engineers, Dallas, TX, 2000.